METHOD ARTICLE

REVISED Antibiotic Drug screening and Image Characterization Toolbox (A.D.I.C.T.): a robust imaging workflow to monitor antibiotic stress response in bacterial cells *in vivo* [version 3; peer review: 2 approved]

Benjamin Mayer[1-3], Meike Schwan[4], Kai M. Thormann[4], Peter L. Graumann[2,3]

[1]Institute of Clinical Pharmacology, Goethe University Frankfurt Am Main, Theodor Stern Kai 7, 60590, Germany
[2]Department of Chemistry, Philipps Universität Marburg, Marburg, Hessen, 35032, Germany
[3]SYNMIKRO, LOEWE Center for Synthetic Microbiology, Marburg, Germany
[4]Institut für Mikrobiologie und Molekularbiologie, Justus-Liebig-Universität Gießen, Gießen, Hessen, 35392, Germany

v3 **First published:** 06 Apr 2021, **10**:277
https://doi.org/10.12688/f1000research.51868.1
Second version: 09 Sep 2021, **10**:277
https://doi.org/10.12688/f1000research.51868.2
Latest published: 17 May 2022, **10**:277
https://doi.org/10.12688/f1000research.51868.3

Abstract

The search for novel drugs that efficiently eliminate prokaryotic pathogens is one of the most urgent health topics of our time. Robust evaluation methods for monitoring the antibiotic stress response in prokaryotes are therefore necessary for developing respective screening strategies. Besides advantages of common *in vitro* techniques, there is a growing demand for *in vivo* information based on imaging techniques that allow to screen antibiotic candidates in a dynamic manner. Gathering information from imaging data in a reproducible manner, robust data processing and analysis workflows demand advanced (semi-)automation and data management to increase reproducibility. Here we demonstrate a versatile and robust semi-automated image acquisition, processing and analysis workflow to investigate bacterial cell morphology in a quantitative manner. The presented workflow, A.D.I.C.T, covers aspects of experimental setup deployment, data acquisition and handling, image processing (e.g. ROI management, data transformation into binary images, background subtraction, filtering, projections) as well as statistical evaluation of the cellular stress response (e.g. shape measurement distributions, cell shape modeling, probability density evaluation of fluorescence imaging micrographs) towards antibiotic-induced stress, obtained from time-course experiments. The imaging workflow is based on regular brightfield images combined with live-cell imaging data gathered from bacteria, in our case from recombinant *Shewanella*

Open Peer Review

Approval Status ✓ ✓

	1	2
version 3 (revision) 17 May 2022		✓ view
version 2 (revision) 09 Sep 2021	✓ view	? view
version 1 06 Apr 2021	? view	

1. **Massimiliano Lucidi**, Roma Tre University, Rome, Italy

2. **Janos Kriston-Vizi**, University College London, London, UK
Qing Hsuan Ong, University College London, London, UK

Any reports and responses or comments on the article can be found at the end of the article.

cells, which are processed as binary images. The model organism expresses target proteins relevant for membrane-biogenesis that are functionally fused to respective fluorescent proteins. Data processing and analysis are based on customized scripts using ImageJ2/FIJI, Celltool and R packages that can be easily reproduced and adapted by users. Summing up, our approach aims at supporting life-scientists to establish their own imaging-pipeline in order to exploit their data as versatile as possible and in a reproducible manner.

Keywords
Combined workflow, ImageJ2, FIJI, cell shape modelling, R-statistics, machine learning, clustering, image processing, image analysis, automation, drug screening

This article is included in the Bioinformatics gateway.

This article is included in the NEUBIAS - the Bioimage Analysts Network gateway.

Corresponding authors: Benjamin Mayer (bmayer@med.uni-frankfurt.de), Peter L. Graumann (peter.graumann@synmikro.uni-marburg.de)

Author roles: Mayer B: Conceptualization, Data Curation, Formal Analysis, Investigation, Methodology, Project Administration, Resources, Software, Validation, Visualization, Writing – Original Draft Preparation, Writing – Review & Editing; **Schwan M**: Conceptualization, Data Curation, Resources, Validation, Writing – Review & Editing; **Thormann KM**: Funding Acquisition, Project Administration, Supervision, Writing – Review & Editing; **Graumann PL**: Funding Acquisition, Project Administration, Supervision, Writing – Review & Editing

Competing interests: No competing interests were disclosed.

Grant information: This work was supported by Deutsche Forschungsgemeinschaft (DFG)-funded Transregio Collaborative Research Center [TRR 174].

How to cite this article: Mayer B, Schwan M, Thormann KM and Graumann PL. **Antibiotic Drug screening and Image Characterization Toolbox (A.D.I.C.T.): a robust imaging workflow to monitor antibiotic stress response in bacterial cells *in vivo* [version 3; peer review: 2 approved]** F1000Research 2022, **10**:277 https://doi.org/10.12688/f1000research.51868.3

First published: 06 Apr 2021, **10**:277 https://doi.org/10.12688/f1000research.51868.1

REVISED **Amendments from Version 2**

Typos corrected. Questions regarding the workflow where updated in Figure 3 to address the reviewer questions. Raw data was added to the osf repository. Figures are annotated according to the image type (brightfield or fluorescence micrograph) that was used. Figure 3 was updated.

Any further responses from the reviewers can be found at the end of the article

Introduction

Bioimage analysis is continuously changing our understanding about the world and how we see our environment. Bacteria are present at µm scale and physiological processes, like cellular signalling events, are even lower than nanometer scale. Cell shape is important for these non-compartmentalized, unicellular organisms. The question of how fast cells grow and divide is connected to tightly regulated intracellular processes like protein-biogenesis from which novel synthesized proteins are translocated along synthesis pathways to their target. Associated proteins play an important role in membrane biogenesis[1–3]. Membrane proteins are synthesized by ribosomes and usually co-translationally inserted into the cytoplasmic membrane. In this process, the signal recognition particle (SRP; composed of SRP RNA and of Ffh protein) recognizes the signal sequence of the nascent polypeptide at the ribosome[4]. This complex is recognized by the SRP receptor FtsY and is delivered to the translocon in the cytoplasmic membrane[5–7]. The nascent polypeptide can be inserted into the membrane or translocated across the membrane by the translocon[8,9]. Disruption of these processes results in dysregulation of essential networks followed by reduced viability, for instance, via chemically induced stress by antibiotic compounds. Susceptibility towards different antibiotics can vary from organism to organism depending on the mode of action of the compound. To further understand respective mechanisms of cellular stress response in bacteria, morphological feature changes are useful to monitor those *in vivo*. Our goal is to illustrate how an imaging based workflow can be efficiently deployed to monitor these processes as part of an antibiotic drug screening strategy involving cell morphology and viability. Furthermore, the presented combined workflow shows how to extract valuable information from imaging data in a reproducible manner using classic statistical approaches, as well as unsupervised machine learning algorithms.

Methods

Biological model system

Our model organism *Shewanella putrefaciens* CN-32 is a Gram-negative bacterium that occurs in aquatic environments[10]. Depending on its growth and division cycles, it has approximately 3 µm in length and 1 µm in width at exponential phase (see Figure 1). Cell division occurs with peak rates at exponential phase represented by OD_{600} 0.5. In our study, we use markerless insertions at the original gene locus functionally expressing fusion-proteins that are relevant for membrane protein-biogenesis: bacterial signal recognition particle Ffh, its receptor FtsY and ribosomal protein of large subunit L1. In order to monitor drug induced stress responses that affect protein-biogenesis, mVenus is used as a fluorescent protein for fluorescence microscopy. Recombinant strains are cultured at 30°C and 200 rpm in Lysogeny broth (LB) medium without antibiotics. This aspect is beneficial to avoid potential bias induced by compound interaction. To analyze antibiotic stress on membrane biogenesis, the protein synthesis inhibitor puromycin was used (200 μg/ml). Puromycin inhibits translation via early termination and subsequent premature release of the nascent polypeptide chain (reviewed by Aviner in 2020)[11,12]. Additionally, RNA-polymerase inhibitor rifampicin (RIF)[13] (25 µg/ml) and peptidyl transferase inhibitor chloramphenicol (CM)[14] (50 µg/ml) were used to confirm outcomes of the deployed workflow[15].

Drug screening strategy

Drug screening time-course replicates are taken at different days. Cells are inoculated from an overnight culture and cultured at 30°C and 200 rpm until OD_{600} 0.5. From this batch, 1 ml is sampled into a glass tube as steady-state (NC), 1 ml treated with antibiotics and is continuously incubated with same conditions. A sample of 3 μl is taken from the culture at steady state and mounted on slides using 1% ultrapure agarose for reduced background. During imaging of cells at steady-state, cells treated with antibiotics are incubated for a minimum of 30 minutes until image acquisition. Similar to this, samples from treated culture after a minimum of 60 minutes are taken accordingly. Viability assay is additionally performed after timecourse experiments. We assume that cells treated with the compound during the time-course experiment are sublethally impaired in cell-growth and division. In order to do so, cells at steady-state and treated with puromycin are 10 fold serially diluted and distributed on LB-agar plates for further incubation at 30°C overnight and imaged using a Fusion-Gel-Illuminator.

Image acquisition

Images are acquired using brightfield and fluorescence microscopy. In our live-cell imaging pipeline, we use an Olympus IX 71 microscope (100x/NA 1.49/optovar 1.6) customized for slimfield microscopy[16] with a fast image acquisition conducted by an Andor iXON Ultra EMCCD camera. Brightfield images are acquired using 50 ms exposure time (see Figure 1). Live-cell time-lapse recordings are acquired using 16 ms exposure time. We take advantage of photobleaching steps through continuous slimfield illumination until single particles can be localized (see Figure 2). Continuous slimfield excitation for photobleaching of the samples is conducted using 514 nm laser line (50%). The microscope setup uses Andor Solis as camera software using at least 2000 frames with integration times of 17.76 ms. Further information about the raw data used in this study is covered in Mayer *et al.*, 2021[15].

Image processing and analysis

Image processing in this workflow is conducted using ImageJ2/FIJI[17–21]. Raw grayscale images sequentially and automatically annotated, transformed from 16-bit into 8-bit, non-linearily noise reduced using a Kuwahara filter and thresholded using 'Percentile'[22] thresholding algorithm and segmented using watershed segmentation for cell detection[23,24] (see Figure 1).'Percentile' is used in this workflow thus initial analysis of processed binary brightfield images showed that

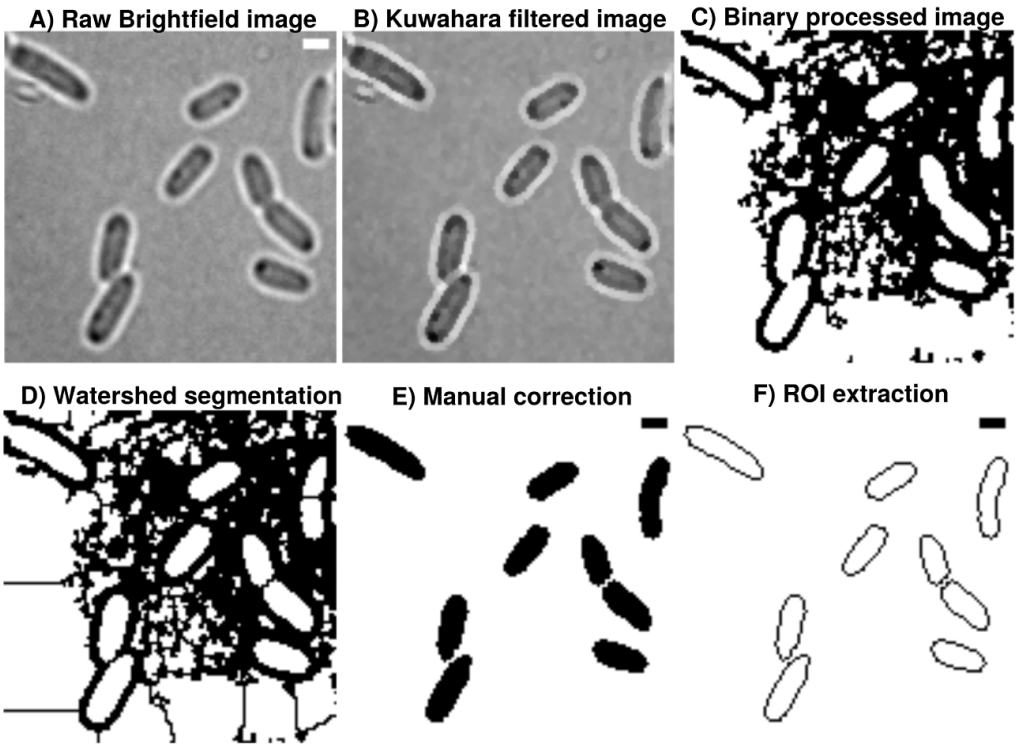

Figure 1. A) Brightfield images are transformed from 16-bit into 8-bit and smoothed by **B**) non-linear noise reduction using the Kuwahara filter option in FIJI (sampling window = 2). Noise reduced images are **C**) thresholded using 'Percentile' thresholding algorithm and **D**) segmented using watershed for cell discrimination. **E**) Resulting binary images are finally corrected manually by correcting potential false positive cells through drawing options. **F**) ROI are extracted from appropriate binary images, stored as individual .zip folders which also involves measurement of cellular areas in an automated manner. This process can be repeated until the the correction is optimal and representative for further analysis. Further analysis always refer to the updated data base and corrections are automatically included when image analysis is reproduced accordingly in Celltool or R-statistics. Scale bar = 1 μm.

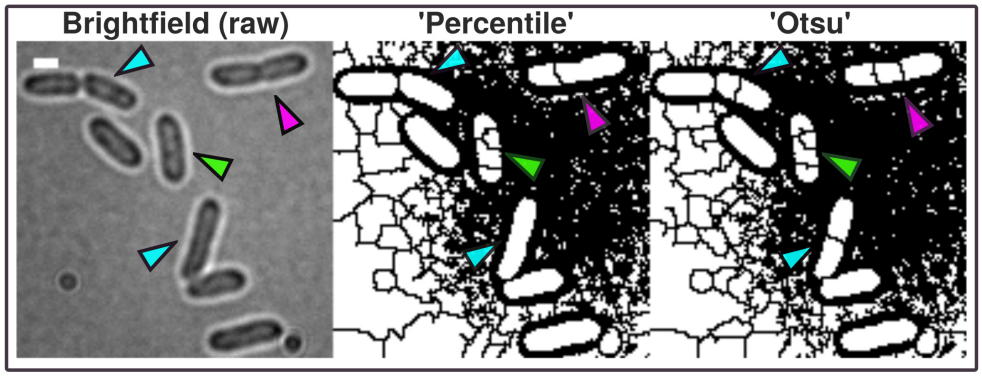

Figure 2. Brightfield image (scale bar = 1 µm) shows Shewanella putrefaciens cells at different cell cycle stages. In contrast to more advanced imaging techniques like phase contrast and Nomarski-microscopy, regular brightfield images are more difficult to process into binary images and resulting ROI possibly need manual correction (green arrow). The A.D.I.C.T. workflow is capable of processing binary images that can be segmented further using watershed segmentation as shown with this study. Although images need to be manually corrected due to the limitation of the imaging technique, cells are thresholded in a more conservative manner due to the use of pixel preserving thresholding algorithm 'Percentile'. 'Otsu' introduces artificial gaps more frequently inside ROI (compare cyan and magenta arrows). Therefore, 'Percentile' is used for this data because it requires less correction. However, 'Otsu' thresholding algorithm is used in the paper to mask fluorescent micrograph projections for measuring intensity.

this thresholding algorithm is more efficient compared to more common algorithms like 'Otsu' (see Figure 2). Resulting binary images are finally corrected manually using the paint function of ImageJ2/FIJI accordingly (see Figure 1). This process can be repeated until the correction is optimal and representative for further analyses (see Figure 3). Fluorescence time lapse recordings are automatically annotated, cropped after sufficient photobleaching steps and projected using the 'Standard deviation' method. This method is used for tomographic representations and highlights areas of high fluorescent densities within a region of interest (ROI). Resulting fluorescence micrographs are background corrected using the math function 'subtract'. All images are automatically scaled and stored in a database management system that is connected through a set of predefined folder operations within the automation script. Regions of interest (ROI) are automatically detected using ImageJ2/FIJI and further processed using scripts based on macro language implemented in ImageJ2/FIJI (see Figure 1). ROIs are extracted from binary images using the ROI-manager plugin and used to create a mask for cell-measures of projected fluorescence micrographs based on the use of 'Otsu' thresholding[25] (see Figure 3).

As a result, we receive comma separated value (.csv) tables that are merged using a custom script in R-statistics based on the 'dplyr' package to organize and merge the tables to a final result-table. Cell shape analysis is conducted using Celltool developed by Pincus lab for cell shape modelling[26]. Scripts for extraction of polygonal contours, alignment, principal component analysis (PCA), statistical evaluation of probability density of cell areas or curvatures and modelling of shape modes are adapted and modified according to the tutorial from Pincus labs (https://zplab.wustl.edu/celltool/). Statistical evaluation of cell areas collected from ROI and fluorescence measurements mean gray value (mgv) as well as integrated density (IntDen) (https://imagej.nih.gov/ij/docs/menus/analyze.html) are statistically analyzed with Rstudio (v.1.1.463) using a customized markdown pipeline in R 3.6.1[27–38]

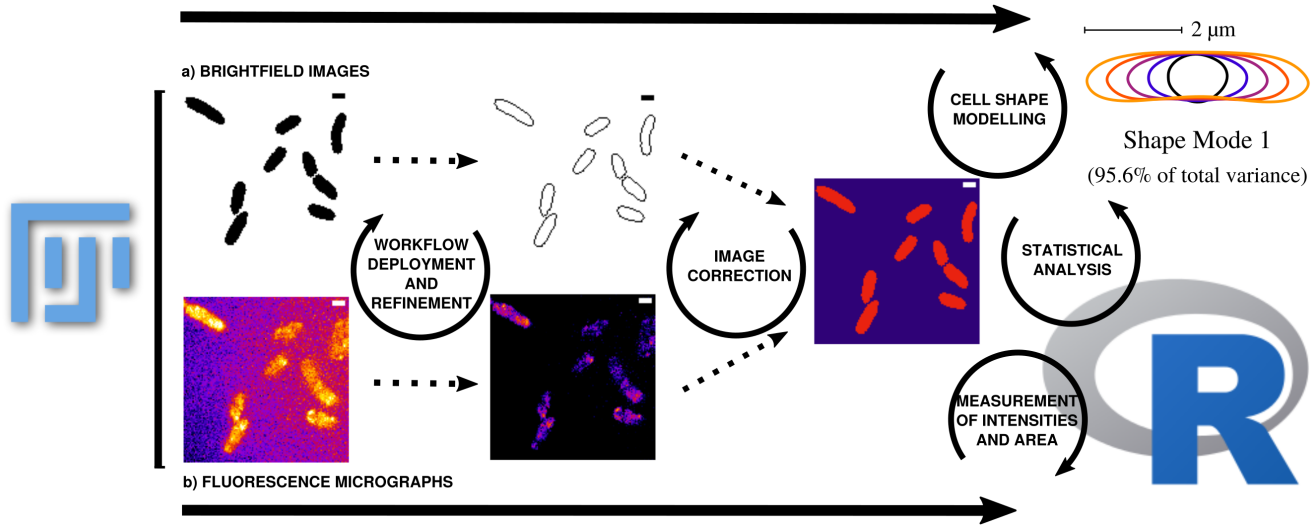

Figure 3. Outline of data processing and analysis steps used in this workflow. Data can be corrected and updated at every stage of the workflow to continuously improve the database until bias is minimized. a) ROIs are collected from binary images that are transformed from raw grayscale brightfield images. The measured area (µm^2) using ImageJ refers to respective ROI and can be compared with the area results from Celltool (Celltool also calculates the area based on the transformed binary image). The measurements collected using the ImageJ function can be further used for area comparison in combination with mean gray values and integrated densities or can be applied as a mask to measure the fluorescence micrographs within the respective cell boundaries. This step eliminates signal that is located outside the ROI. b) Processing of the fluorescence time lapse recordings is conducted on the basis of cropping the relevant frames after sufficient photobleaching until single particle level is reached. Analysis of fluorescence micrographs is based on the measurements defined in ImageJ macros and then further processed using an R pipeline using the mentioned packages. Fluorescence micrographs that are used to measure intensities refer to the respective protein and cell vitality monitored over time. It is important to know that the raw data does not contain useful meta-data by scratch. The workflow enables the experimenter to fully control the annotation of the data in a reproducible way. The outcome should be that after the workflow (re-)deployment of the processing using the fluorescence micrographs, properly annotated data tables that can be combined for further analysis using R-packages are obtained. Intensity measurements directly correspond to protein levels and dynamics. Data can be therefore used to obtain more detailed perspectives about the observed biological process. Cellular stress can be monitored with different variables containing information for fluorescence activity and morphological changes during stress induction. To monitor the same data from different perspectives makes the analysis more robust and allows to explore the cellular stress response in a more detailed, simultaneous and semi-automated manner. This also helps to re-evaluate the analysis in a well documented manner thus the extraction of information and the processing starts from the raw data (brightfield and fluorescence micrographs). Further modeling for instance becomes easier thus data is well prepared for more complex analysis tasks. Taken together, the workflow allows to evaluate the observed cellular stress response at protein expression levels (fluorescence microscopy) in a simultanous and interconnectd (ROIs based on brightfield images) manner with stress response observed by cell shape abnormalities (Celltool). Scale bar = 1 μm.

(see Figure 3). To understand the context between mgv and IntDen, it is important to know that:

$$\text{Mean Gray Value} = \frac{\text{Gray values (selection)}}{\text{pixel number}}$$

$$\text{Integrated Density} = \text{Mean Gray Value} \times \text{Area}\,(\mu m^2)$$

Statistical distributions resulting from measurements are tested for normality using the Shapiro-Wilk test[39]. Non-parametric Wilcoxon rank sum test is used to test pairwise for significance (confidence level: 0.95 ; $p < 0.05$ = * ; $p < 0.01$ = ** ; $p < 0.001$ = ***)[40,41]. In order to establish an unsupervised machine learning approach using the ImageJ2/FIJI results tables, Density based clustering of applications with noise (dbscan) R-package is applied to cellular areas and mean gray value with the aim to evaluate clusters that distinguish between cellular amount of fusion proteins (indicated by fluorescence) and cellular areas[42].

Proof of concept

Cell shape analysis and modelling

Puromycin treated cells show abnormal cell morphology regarding their size and shape over time (see Figure 4A). Cell shape changes can be modelled with Celltool. Generalized models according to time points show increased variation of cells explained by shape mode 1, 2 and 3 (see Figure 5), if stressed with puromycin. Corresponding to these findings, probability plots show increasing cell size (see Figure 4C) and abnormal cell morphology reflected by normalized curvature in a quantitative manner during induction with puromycin (see Figure 4D). During progression of the time-course, cell length increases which indicates cell division stress which was also shown by other groups before[43,44]. Corresponding to that, Celltool analysis under rifampicin and chloramphenicol induced stress shows similar outcomes (see Figure 6). Differences between cellular areas grouped by condition times show clearly a significant time dependent increase (see Figures 7A and B). Although differences of cellular areas appear to be significant as well between L1, Ffh and FtsY if grouped by respective strains, there is no significant difference between Ffh and FtsY. Furthermore, these findings are strongly influenced by extreme values suggesting that these differences are not a result due to puromycin (see Figures 7C and D). The fluorescence intensity of Ffh and FtsY decreases over time because no new proteins can be translated caused by the protein synthesis inhibitor puromycin and the old proteins are degraded (see Figure 7E and F). From here, it can be only speculated why L1 amount is higher after 30 minutes of induction. One possible explanation could be that the compound does not affect

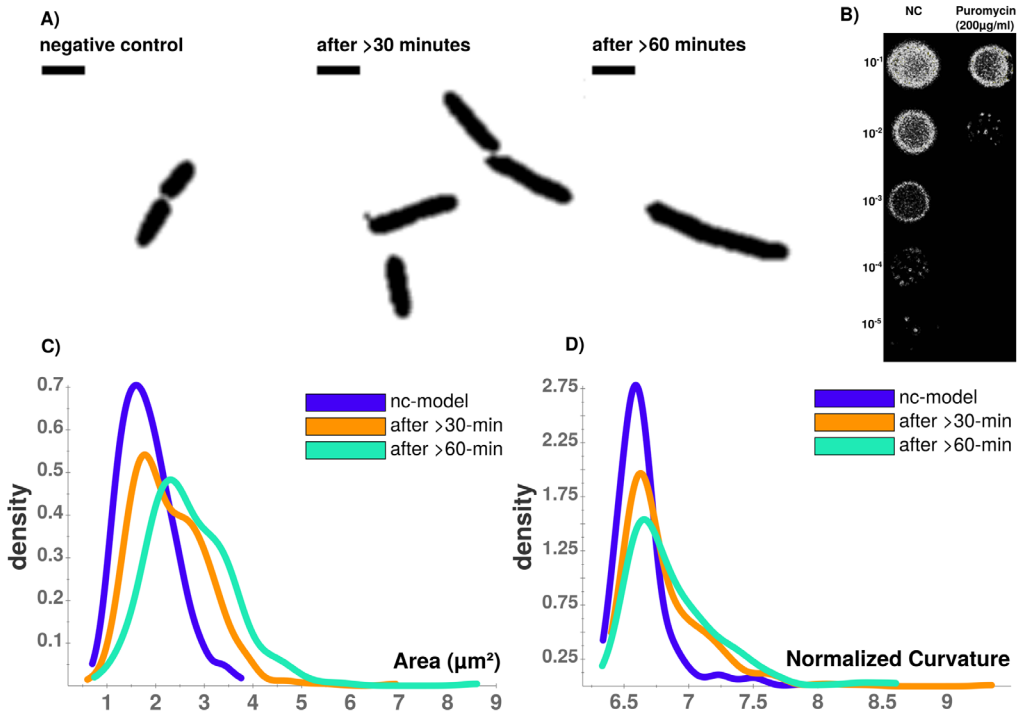

Figure 4. Brightfield image analysis using Celltool. A) Time-course of puromycin stressed cells at different time points (NC, after >30 min., after >60 min. Viability assay with unstressed (NC) and puromycin stressed cells. **B**) Colonies on LB-agar show drastic effects between serial dilutions of steady-state and puromycin treated cells. Whilst viability is not impaired for steady-state, protein biosynthesis inhibitor puromycin shows sublethal impaired cell growth and division indicated by reduced colony density. **C**) Celltool area comparison shows increasing numbers of larger cells that can be quantified which corresponds to **D**) an increasingly abnormal cell curvature over time after puromycin induced stress. Scale bar = 2 μm.

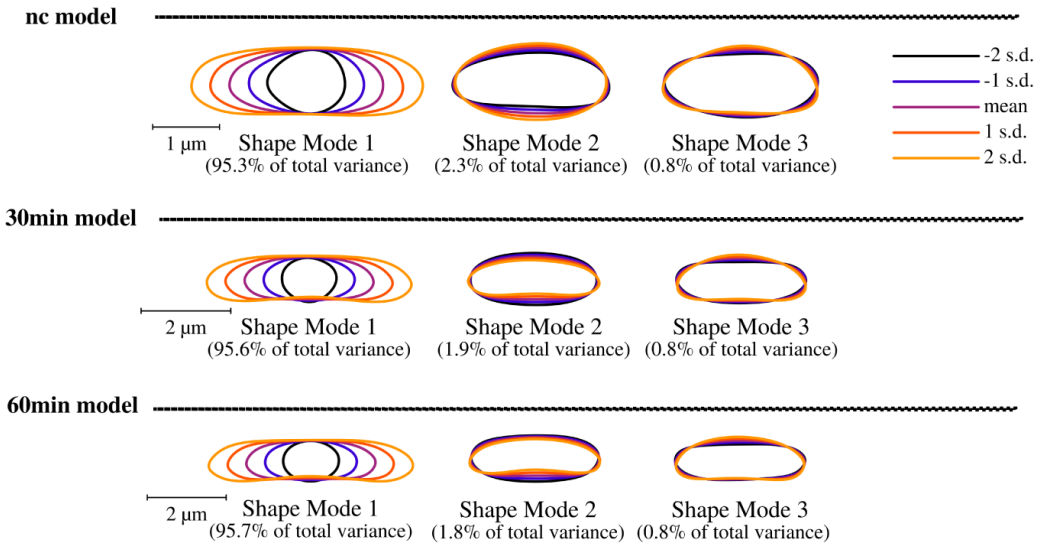

Figure 5. Celltool extraction and modeling of time course imaging results shows generalized model based on its shape variation. Brightfield image analysis using Celltool. Lower limits of explained differences of shape models caused by variation are taken into consideration if not lower than 0.8%. Our results suggest for all time-course acquisitions that mode 1 explains the majority of variation followed by width of the cells represented by mode 2 and 3. Considering the scale bar, the generalized models clearly show that puromycin is indeed affecting the cell length specifically thus cell division might be impaired. These findings correspond to the analysis of cellular areas and curvatures.

ribosome formation itself. Furthermore, the autocatalytic nature of the ribosomes makes it even more complicated to address[45]. However, the increased integrated density (see Figure 7F) indicates that changes of the cellular area (in 2D space of course, which is actually a volumetric aspect in 3D) is the decisive parameter to monitor puromycin stress response in our approach. Our assumption that the cellular area is indeed the relevant indicator for puromycin induced stress is further supported by the fact that comparison of cellular areas and curvature with Celltool corresponds to the R-statistics analysis.

Clustering

Results for cluster analysis show that intensity measurements are less powerful to uncover antibiotic stress response in our study compared to abnormal cell grow represented by increased cellular area (see Figure 8). For L1, 6 distinct clusters are identified to which the highest mgv is close beyond 2500 mgv (shown in green). No cell beyond a mgv of 2000 has a larger cellular area than 4 μm^2 (see Figure 8 L1). This possibly indicates that higher mgv refers to a non-homogenously distributed population of cells with high L1 amount. It further supports the idea that abnormal cell shape and increased cellular area over time are the relevant indicators for monitoring puromycin induced stress response (see Figure 4, Figure 5, Figure 6, Figure 7). In contrast to L1, Ffh shows 10 clusters and FtsY 3 clusters. L1 (red), Ffh (red) and FtsY (green) show one central cluster. However, key finding of the cluster analysis is that cells of respective high protein amount have no enlarged cellular area beyond 4 μm^2 for all investigated proteins. It confirms that stressed cells (indicated by enlarged cellular area) do not correspond to increased intensity measurements (compare to Figure 7E and F).

Conclusions

The A.D.I.C.T. workflow is sensitive enough to monitor time-course drug-screening experiments in a reproducible manner. Binary images are very robust regarding their information content and useful for addressing complex questions involving cell shape modelling at nanoscale levels. However, binary images processed in this study are based on brightfield images and extended manual correction is necessary (see Figure 1). By using more powerful techniques like phase-contrast or specific membrane stains for instance, cell detection would be improved and the effort to manually correct binary images could be decreased further resulting in almost fully automated cell detection. Nevertheless, although we applied very basic image acquisition techniques, it is clearly demonstrated that cell division specific events can be monitored, processed and analyzed using the presented workflow. The advantage of the workflow is that every step can be redeployed and improved starting from the raw data processing to final statistical evaluation using high-level or low-level programming languages. Bias can be reduced by re-deployment and refinement of the database

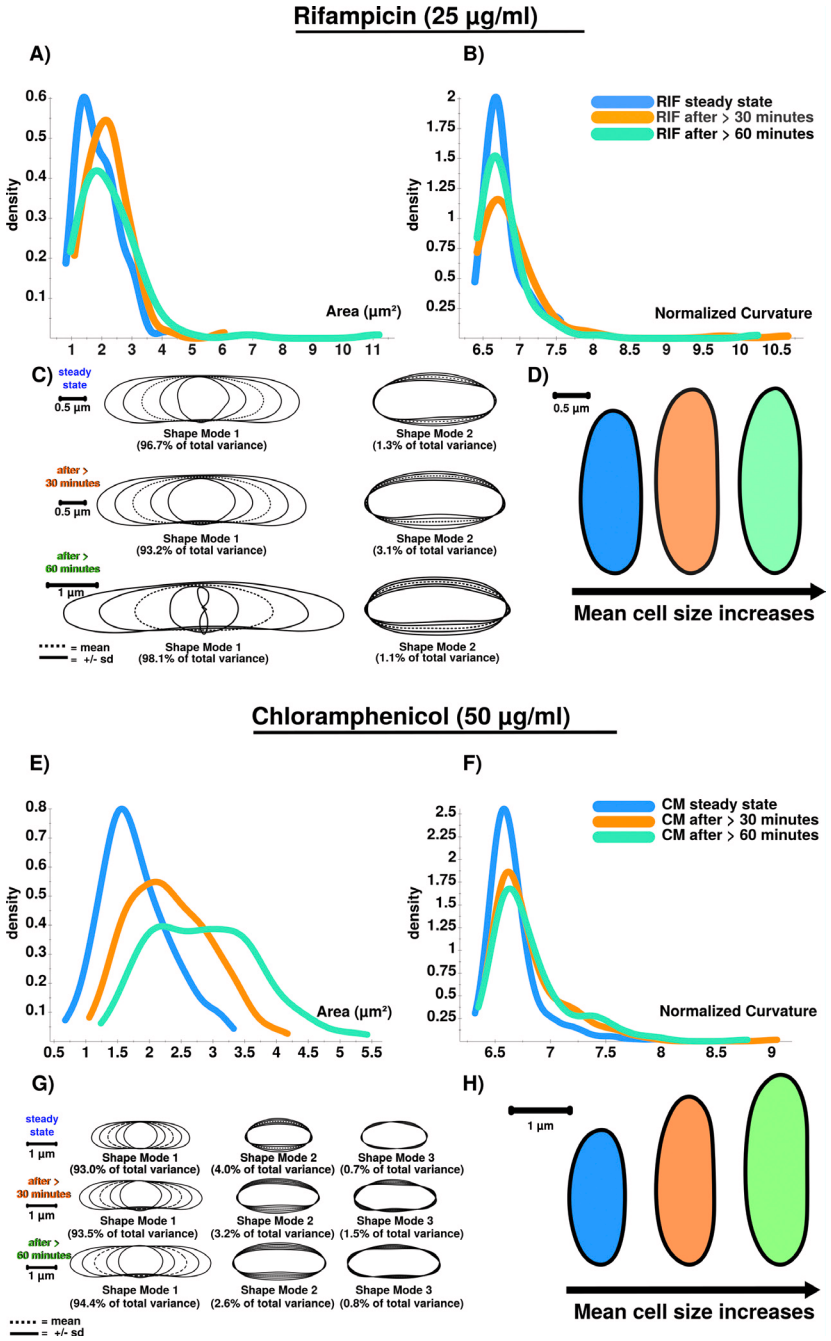

Figure 6. Brightfield image analysis using Celltool. A) RIF stressed cells show increased cellular area over time. **B**) Curvatures for analyzed cellular populations are also increased after RIF stress is induced. However, curvature does only increase in total after stress induction, and not successively. Curvature is stronger affected after 30 minutes (orange) compared to conditions after 60 minutes (green), which could be triggered by an initial shock induced by RIF. **C**) PCA results confirm the stress response using shape mode 1 and 2. RIF stressed cells show a high variability regarding cell length. This is why the shape mode 1 after 60 minutes (green) is difficult to model (see the inner shape of mode 1 (-2 s.d.)). Remarkably, RIF stress induces division stress according to our results, indicated by abnormally enlarged cells. **D**) Extracted and compared mean cell shapes indicate that RIF stressed cells tend to be larger compared to steady-state cells and show that the stress-response is detectable at 25 µg/ml. **E**) CM stressed cells show increased cellular area over time. **F**) Curvatures for analyzed cellular populations are increased after CM stress induction. Similar to RIF (see Figure 6B) curvature does only increase in total but not successively. **G**) PCA results confirm the stress response using shape mode 1, 2 and 3. CM induced stress results in a higher number of abnormally shaped cells. **H**) Extracted and compared mean cell shapes (mode 1) show that cells are successively enlarged during time courses compared to steady-state cells on average.

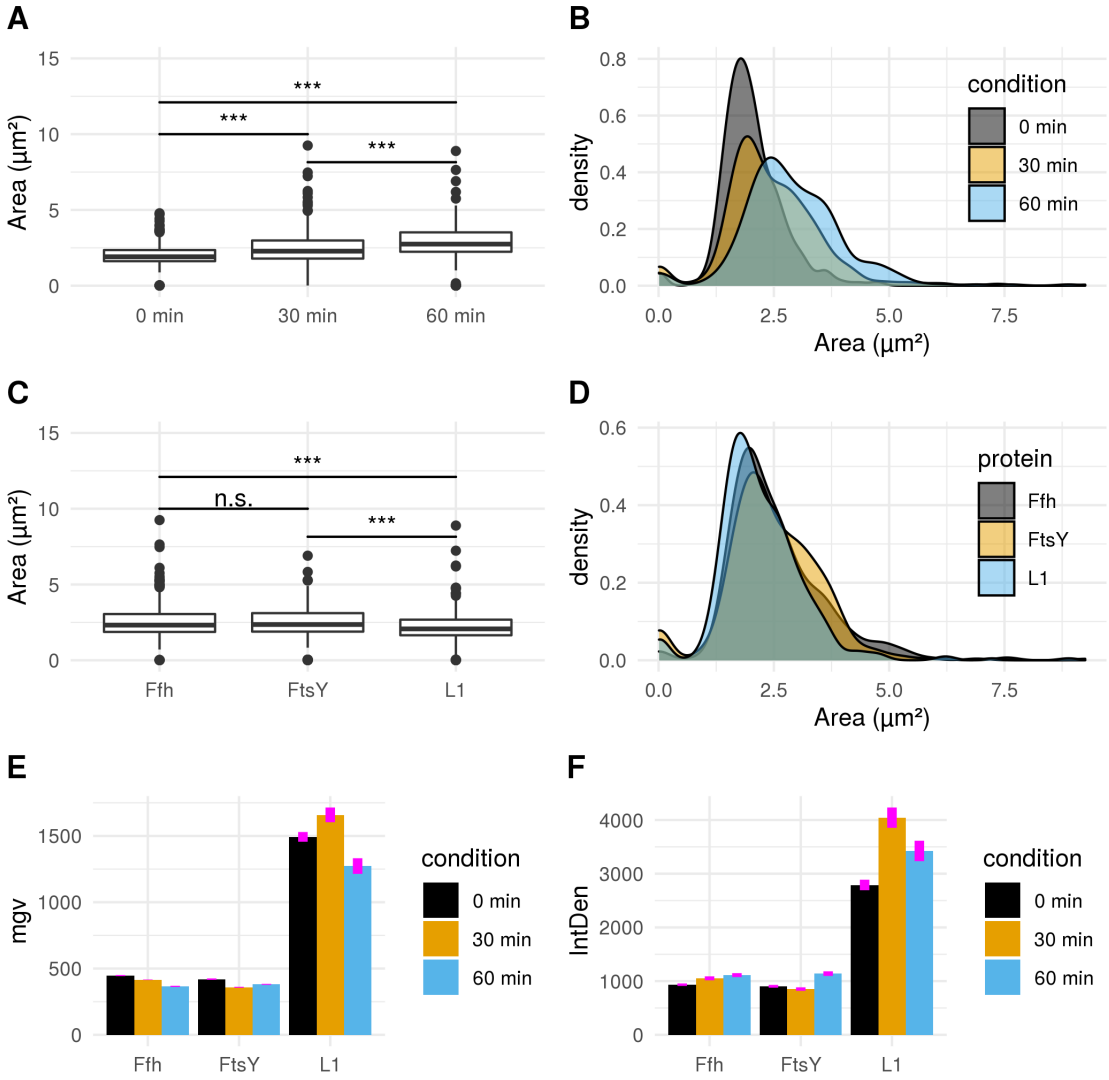

Figure 7. Fluorescence micrograph analysis of intensity measurements compared to areas defined by ROIs. A) Boxplot comparison shows increased cell size distribution for all observed fusion proteins over time if stressed with puromycin (0 min: n = 412; 30 min: n = 455; 60 min: n = 338). Extreme value count increases over time for the pooled fusion protein samples. **B**) Probability density of larger cells increases over time for pooled fusion proteins. Results show decreasing number of cells with smaller area indicating that puromycin induced stress results in increase of larger cells for the whole sample. **C**) Cellular areas grouped according to respective strains containing different fusion proteins are differing: Ffh: n = 453; FtsY: n = 371; L1: n = 381. **D**) Probability density plot does not indicate a strong difference if compared between strains of different fusion proteins. **E**) Comparison of mean gray values (mgv) between groups of fusion proteins show slightly decreasing effects over time for Ffh (0 min: n = 131; 30 min: n = 184; 60 min: n = 138) and FtsY (0 min: n = 112; 30 min: n = 160; 60 min: n = 99). L1 (n = 169) appears to increase after 30 min (n = 111) of stress-induction followed by a strong decrease after 60 min (n = 101). Error bars refer to standard error (se). **F**) Integrated density (IntDen) comparison between monitored proteins over time show increasing tendencies over time for Ffh and FtsY. L1 increases after 30 min and decreases after 60 min. Thus IntDen is directly influenced by the area of the cells, it is plausible that IntDen show an overall increase over time compared to mgv, which is not influenced by the cellular area. Error bars refer to standard error (se).

which enhances reproducible dissection and analysis of complex data sets in an automated fashion. The amount of useful information gathered from deploying the A.D.I.C.T. workflow in case of puromycin stress on our model organism is convincing but far away from being fully covered by this article. To sum up, our approach illustrates how powerful very basic

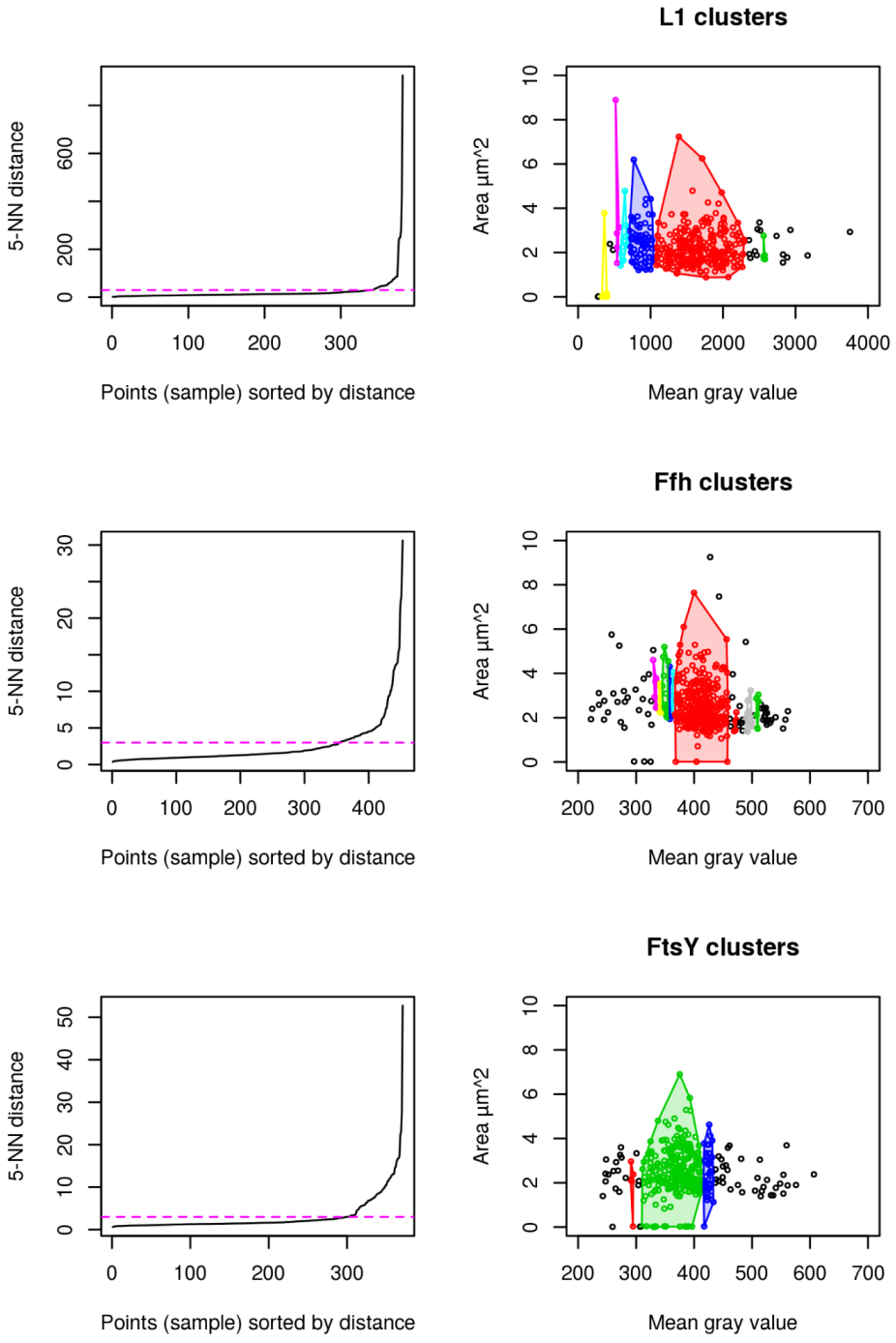

Figure 8. Fluorescence micrograph analysis using DBSCAN cluster analysis. L1 (n = 381), Ffh (n = 453) and FtsY (n = 371) shows that the cells with largest area do not belong to the cells with the highest amount of protein. 5-Nearest Neighbors (NN) distance plots are used to define the appropriate epsilon values for dbscan and are adjusted manually according to knee of the curve (magenta). Resulting clusters are color coded for discrimination respectively (right).

imaging techniques can be, if applied with a robust, combined workflow and we hope that it empowers other researchers to take advantage from it for their own research tasks.

Data availability

Open Science Framework: Test data for A.D.I.C.T. workflow, https://osf.io/ynkz3/[46]

This project contains the following files:

- Binary images
- Projections
- ROI
- merged results tables (.csv)
- brightfield raw images
- time-lapse raw recordings

Scripts from this study are available at Github: https://github.com/Image-processing-and-analysis-workflows/A.D.I.C.T.

Archived scripts as at time of publication: https://doi.org/10.5281/zenodo.5342923[47]

License: GNU GPL 3.0

Acknowledgements

This publication was supported by COST Action NEUBIAS (CA15124), funded by COST (European Cooperation in Science and Technology).

References

1. Walter P, Blobel G: **Signal recognition particle: a ribonucleoprotein required for cotranslational translocation of proteins, isolation and properties.** *Methods Enzymol.* 1983; **96**: 682–91.
PubMed Abstract | Publisher Full Text

2. Seluanov A, Bibi E: **Ftsy, the prokaryotic signal recognition particle receptor homologue, is essential for biogenesis of membrane proteins.** *J Biol Chem.* 1997; **272**(4): 2053–5.
PubMed Abstract | Publisher Full Text

3. Peschke M, Le Goff M, Koningstein GM, *et al.*: **Srp, ftsy, dnak and yidc are required for the biogenesis of the *e. coli* tail-anchored membrane proteins djlc and flk.** *J Mol Biol.* 2018; **430**(3): 389–403.
PubMed Abstract | Publisher Full Text

4. Luirink J, High S, Wood H, *et al.*: **Signal-sequence recognition by an *escherichia coli* ribonucleoprotein complex.** *Nature.* 1992; **359**(6397): 741–3.
PubMed Abstract | Publisher Full Text

5. Herskovits AA, Bibi E: **Association of *escherichia coli* ribosomes with the inner membrane requires the signal recognition particle receptor but is independent of the signal recognition particle.** *Proc Natl Acad Sci U S A.* 2000; **97**(9): 4621–6.
PubMed Abstract | Publisher Full Text | Free Full Text

6. Draycheva A, Bornemann T, Ryazanov S, *et al.*: **The bacterial srp receptor, ftsy, is activated on binding to the translocon.** *Mol Microbiol.* 2016; **102**(1): 152–67.
PubMed Abstract | Publisher Full Text

7. Jomaa A, Boehringer D, Leibundgut M, *et al.*: **Structures of the *e. coli* translating ribosome with srp and its receptor and with the translocon.** *Nat Commun.* 2016; **7**: 10471.
PubMed Abstract | Publisher Full Text | Free Full Text

8. Draycheva A, Lee S, Wintermeyer W: **Cotranslational protein targeting to the membrane: Nascent-chain transfer in a quaternary complex formed at the translocon.** *Sci Rep.* 2018; **8**(1): 9922.
PubMed Abstract | Publisher Full Text | Free Full Text

9. Kuhn P, Draycheva A, Vogt A, *et al.*: **Ribosome binding induces repositioning of the signal recognition particle receptor on the translocon.** *J Cell Biol.* 2015; **211**(1): 91–104.
PubMed Abstract | Publisher Full Text | Free Full Text

10. Fredrickson JK, Zachara JM, Kennedy DW, *et al.*: **Biogenic iron mineralization accompanying the dissimilatory reduction of hydrous ferric oxide by a groundwater bacterium.** *Geochim Cosmochim Acta.* 1998; **62**(19–20): 3239–3257.
Publisher Full Text

11. Yarmolinsky MB, Haba GL: **Inhibition by puromycin of amino acid incorporation into protein.** *Proc Natl Acad Sci U S A.* 1959; **45**(12): 1721–1729.
PubMed Abstract | Publisher Full Text | Free Full Text

12. Aviner R: **The science of puromycin: From studies of ribosome function to applications in biotechnology.** *Comput Struct Biotechnol J.* 2020; **18**: 1074–1083.
PubMed Abstract | Publisher Full Text | Free Full Text

13. Campbell EA, Korzheva N, Mustaev A, *et al.*: **Structural Mechanism for Rifampicin Inhibition of Bacterial RNA Polymerase.** *Cell.* 2001; **104**(6): 901–912.
PubMed Abstract | Publisher Full Text

14. Drainas D, Kalpaxis DL, Coutsogeorgopoulos C: **Inhibition of ribosomal peptidyltransferase by chloramphenicol. Kinetic studies.** *Eur J Biochem.* 1987; **164**(1): 53–8.
PubMed Abstract | Publisher Full Text

15. Mayer B, Schwan M, Oviedo-Bocanegra LM, *et al.*: **Dynamics of Bacterial Signal Recognition Particle at a Single Molecule Level.** *Front Microbiol.* 2021; **12**: 663747.
PubMed Abstract | Publisher Full Text | Free Full Text

16. Plank M, Wadhams GH, Leake MC: **Millisecond timescale slimfield imaging and automated quantification of single fluorescent protein molecules for use in probing complex biological processes.** *Integr Biol (Camb).* 2009; **1**(10): 602–612.
PubMed Abstract | Publisher Full Text

17. Schindelin J, Arganda-Carreras I, Frise E, *et al.*: **Fiji: an open-source platform for biological-image analysis.** *Nat Methods.* 2012; **9**(7): 676–82.
PubMed Abstract | Publisher Full Text | Free Full Text

18. Schindelin J, Rueden CT, Hiner MC, *et al.*: **The imagej ecosystem: An open platform for biomedical image analysis.** *Mol Reprod Dev.* 2015; **82**(7–8): 518–29.
PubMed Abstract | Publisher Full Text | Free Full Text

19. Rueden CT, Schindelin J, Hiner MC, *et al.*: **Imagej2: Imagej for the next generation of scientific image data.** *BMC Bioinformatics.* 2017; **18**(1): 529.
PubMed Abstract | Publisher Full Text | Free Full Text

20. Schneider CA, Rasband WS, Eliceiri KW: **NIH Image to ImageJ: 25 years of image analysis.** *Nat Methods.* 2012; **9**(7): 671–675.
PubMed Abstract | Publisher Full Text | Free Full Text

21. Linkert M, Rueden CT, Allan C, *et al.*: **Metadata matters: access to image data in the real world.** *J Cell Biol.* 2010; **189**(5): 777–782.
PubMed Abstract | Publisher Full Text | Free Full Text

22. Doyle W: **Operations Useful for Similarity-Invariant Pattern Recognition.** *Journal of the ACM.* 1962; **9**(2): 259–267.
Publisher Full Text

23. Legland D, Arganda-Carreras I, Andrey P: **MorphoLibJ: integrated library and plugins for mathematical morphology with ImageJ.** *Bioinformatics.* 2016; **32**(22): 3532–3534.
PubMed Abstract | Publisher Full Text

24. Soille P, Vincent LM: **Determining watersheds in digital pictures via flooding simulations**. In M. Kunt (Ed.), *Visual Communications and Image Processing '90: Fifth in a Series*. SPIE. 1990; **1360**.
Publisher Full Text

25. Otsu N: **A Threshold Selection Method from Gray-Level Histograms.** *IEEE Trans Syst Man Cybern Syst.* 1979; **9**(1): 62–66.
Publisher Full Text

26. Pincus Z, Theriot JA: **Comparison of quantitative methods for cell-shape analysis.** *J Microsc.* 2007; **227**(Pt 2): 140–156.
PubMed Abstract | Publisher Full Text

27. R Core Team: **R: A Language and Environment for Statistical Computing.** R Foundation for Statistical Computing, Vienna, Austria, 2019.
Reference Source

28. RStudio Team: **RStudio: Integrated Development Environment for R.** RStudio, PBC., Boston, MA, 2020.
Reference Source

29. Xie Y: **knitr: A General-Purpose Package for Dynamic Report Generation in**

R. R package version 1.31. 2021.
Reference Source

30. Wickham H, François R, Henry L, *et al.*: **dplyr: A Grammar of Data Manipulation.** R package version 1.0.4. 2021.
Reference Source

31. Wickham H: **ggplot2: Elegant Graphics for Data Analysis.** Springer-Verlag New York, 2016.
Reference Source

32. Wickham H, Averick M, Bryan J, *et al.*: **Welcome to the tidyverse.** *J Open Source Softw.* 2019; **4**(43): 1686.
Publisher Full Text

33. Ahlmann-Eltze C: **ggsignif: Significance Brackets for 'ggplot2'.** R package version 0.6.0. 2019.
Reference Source

34. Arnold JB: **ggthemes: Extra Themes, Scales and Geoms for 'ggplot2'.** R package version 4.2.4. 2021.
Reference Source

35. Morales M, with code developed by the R Development Core Team, with general advice from the R-help listserv community, *et al.*: **sciplot: Scientific Graphing Functions for Factorial Designs.** R package version 1.2-0. 2020.
Reference Source

36. Allaire JJ, Xie Y, McPherson J, *et al.*: **rmarkdown: Dynamic Documents for R.** R package version 2.6. 2020.
Reference Source

37. Wilke CO: **cowplot: Streamlined Plot Theme and Plot Annotations for 'ggplot2'.** R package version 1.1.1. 2020.
Reference Source

38. Wickham H, Hester J: **readr: Read Rectangular Text Data.** R package version 1.4.0. 2020.
Reference Source

39. Shapiro SS, Wilk MB: **An Analysis of Variance Test for Normality (Complete Samples).** *Biometrika.* 1965; **52**(3/4): 591–611.
Publisher Full Text

40. Wilcoxon F: **Individual Comparisons by Ranking Methods.** *Biometrics Bulletin.* 1945; **1**(6): 80–83.
Publisher Full Text

41. Mann HB, Whitney DR: **On a Test of Whether one of Two Random Variables is Stochastically Larger than the Other.** *Ann Math Statist.* 1947; **18**(1): 50–60.
Publisher Full Text

42. Hahsler M, Piekenbrock M, Doran D: **dbscan: Fast density-based clustering with R.** *J Stat Softw.* 2019; **91**(1): 1–30.
Publisher Full Text

43. Htoo HH, Brumage L, Chaikeeratisak V, *et al.*: **Bacterial Cytological Profiling as a Tool To Study Mechanisms of Action of Antibiotics That Are Active against *Acinetobacter baumannii*.** *Antimicrob Agents Chemother.* 2019; **63**(4): e02310–18.
PubMed Abstract | Publisher Full Text | Free Full Text

44. Nonejuie P, Burkart M, Pogliano K, *et al.*: **Bacterial cytological profiling rapidly identifies the cellular pathways targeted by antibacterial molecules.** *Proc Natl Acad Sci U S A.* 2013; **110**(40): 16169–74.
PubMed Abstract | Publisher Full Text | Free Full Text

45. Reuveni S, Ehrenberg M, Paulsson J: **Ribosomes are optimized for autocatalytic production.** *Nature.* 2017; **547**(7663): 293–297.
PubMed Abstract | Publisher Full Text | Free Full Text

46. Mayer B, Schwan M, Thormann KM, *et al.*: **Antibiotic Drug screening and Image Characterization Toolbox (A.D.I.C.T.): test data for workflow deployment and reproduction.** 2021.
https://osf.io/ynkz3

47. Mayer B: **A.D.I.C.T. v1.0.4 (v1.0.4).** *Zenodo.* 2021.
http://www.doi.org/10.5281/zenodo.5342923

Open Peer Review

Current Peer Review Status: ✔ ✔

Version 3

Reviewer Report 08 June 2022

https://doi.org/10.5256/f1000research.133641.r138118

✔ **Janos Kriston-Vizi**
Bioinformatics Image Core (BIONIC), MRC Laboratory for Molecular Cell Biology, University College London, London, UK

Qing Hsuan Ong
University College London, London, UK

The author addressed our points with the response, thanks.

Competing Interests: No competing interests were disclosed.

Reviewer Expertise: Bioimage informatics, high-content analysis, high-content screening, quantitative cell biology.

We confirm that we have read this submission and believe that we have an appropriate level of expertise to confirm that it is of an acceptable scientific standard.

Version 2

Reviewer Report 02 March 2022

https://doi.org/10.5256/f1000research.77023.r123723

? **Janos Kriston-Vizi**
Bioinformatics Image Core (BIONIC), MRC Laboratory for Molecular Cell Biology, University

College London, London, UK

Qing Hsuan Ong
University College London, London, UK

The paper titled as Antibiotic Drug screening and Image Characterization Toolbox (A.D.I.C.T.): a robust imaging workflow to monitor antibiotic stress response in bacterial cells in vivo by Mayer *et al*. reports an image acquisition, processing and analysis workflow to investigate quantitative bacterial cell morphology. The presented workflow includes data acquisition, brightfield image processing with ImageJ/Fiji and statistical data analysis with R.

A robust automated image processing workflow of high-content brightfield microscopy image dataset is an interesting topic for the community. The authors choice of open-source software ImageJ/Fiji and R is favourable for the academic community as it supports code transparency re-use and reproducibility. The well-commented image processing script is published in the GitHub repository, which adds value to the paper.

However, the paper only partially delivers the high expectations. The image processing is a 3 steps process: (1) preprocessing using Kuwahara filter, (2) segmentation by calculating the threshold with Percentile algorithm, (3) split virtually merged objects based on concave morphology detection by watershed algorithm.

Major revisions

The limited precision of the Kuwahara-Percentile-Watershed image processing workflow requires the introduction of an additional manual correction step.

- pp5. "Resulting binary images are finally corrected manually using the paint function of ImageJ2/FIJI accordingly".

- Fig 1. "E) Resulting binary images are finally corrected manually by correcting potential false positive cells through drawing options."

- Fig 2. "Although images need to be manually corrected..."

- pp10. "extended manual correction is necessary"

The need for this manual correction of segmentation can be a major limitation of the usability of the workflow for high-content analysis. This limitation is mentioned only marginally. It should be discussed adequately by addressing the following questions:

1. How many images did the screen contain?

2. How many working hours the manual segmentation correction required for the entire image dataset of the screen?

3. Both brightfield and fluorescence images were used in this study. However, it is not clear if brightfield and/or fluorescence images were quantified in figures 3-8. It should be mentioned in figure 3-8 captions which set of raw images (brightfield or fluorescence time-lapse recording) did the data come from.

4. pp5. "Binary images are sequentially" - The image processing pipeline suggests that the sentence must be clarified logically, e.g. replace "Binary images" term with "Raw grayscale images" term.

5. The paper needs more clarification on the image processing and analysis workflow of the fluorescence time lapse images.

6. The role of photobleaching needs to be explained.

7. Only sample raw images are made available. Not all screening image source data underlying the results are available to ensure full reproducibility.

Minor revisions

- pp5. "ROIs are extracted from binary images..." - This sentence needs clarification, the "use of 'Otsu' thresholding" is unclear.

- pp5. Figure 3. - A dotted arrow seems missing between the top left panel and the right one next to it.

Typos

- pp5. "corrected using the math function 'substract'." - Correct 'substract' to 'subtract'.

Is the rationale for developing the new method (or application) clearly explained?

Yes

Is the description of the method technically sound?

Yes

Are sufficient details provided to allow replication of the method development and its use by others?

Partly

If any results are presented, are all the source data underlying the results available to ensure full reproducibility?

Partly

Are the conclusions about the method and its performance adequately supported by the findings presented in the article?

Yes

Competing Interests: No competing interests were disclosed.

Reviewer Expertise: Bioimage informatics, high-content analysis, cell biology.

We confirm that we have read this submission and believe that we have an appropriate level of expertise to confirm that it is of an acceptable scientific standard, however we have significant reservations, as outlined above.

Author Response 29 Apr 2022

Benjamin Mayer, Philipps Universität Marburg, Marburg, Germany

First of all, thank you for the revision of this work. We hope that we can address your points with the following response:

Although not primarily designed for HCS screening, the usability of the workflow for respective approaches needs clarification. The initial idea was to design a very basic approach that can be easily reproduced by a biologically focused group working on cell-morphology. Therefore, brightfield imaging was used. Fluorescence micrographs can be used to generate more detailed cellular representations, but the general idea was to show how to design a basic imaging pipeline with equipment everyone can use. For this study, moving forward towards creating binary images from fluorescence micrographs is an option but beyond the scope of this work. The primary goal of the workflow is, however, to reduce inconsistencies caused by the experimenter through a streamlined data processing and analysis pipeline that can be fully accessed at every stage of the workflow. To judge whether a cell is divided or not is a source of potential inconsistency harboring the risk of excessive variance, depending on respective impressions by the experimenter. However, the main goal of the workflow is to reduce inconsistencies by maintenance of a documented data basis. Decisions that lead to exclusion of cells that are judged as incorrect (or accidentally not included although correct) can be updated towards re- or disintegration of respective cells within the data basis. The way, how the data basis is processed and analyzed is then updated accordingly. Although HCS was not the primary goal, criteria that are necessary to conduct this would involve different approaches regarding the image quality. In contrast to brightfield imaging, super-resolution imaging offers more possibilities to do so. However, also SR imaging can be affected by technical limitations that might need manual correction. Regarding the presented workflow, also images with better quality that need less correction are possibly better suited for a HCS screen. They could be processed and analyzed with the scripts of this workflow after few modifications.

##########
1. How many images did the screen contain?
##########

The puromycin data set contains brightfield images for:

Ffh steady state: 30
Ffh after 30 minutes of induction: 32
Ffh after 60 minutes of induction: 43

FtsY steady state: 33
FtsY after 30 minutes of induction: 36
FtsY after 60 minutes of induction: 35

L1 steady state: 29
L1 after 30 minutes of induction: 22
L1 after 60 minutes of induction: 26

The same number of image sequences that contain the fluorescence images apply accordingly.

The data set for additional controls using rifampicin (89) and chloramphenicol (79) are only used to confirm Celltool results.

##########
2. How many working hours the manual segmentation correction required for the entire image data set of the screen?
##########

The manual correction can be conducted approximately within one or two working days for the data set by a trained person. Using drawing tools in IJ allows to quickly eliminate content outside the ROI. However, aim of this workflow is to access these processing steps at every stage if correction of a cell needs attention in order to refine the data set. Thus all downstream processing and analysis of a data basis depends on the maintenance of the data basis, changes are best applied upstream by making decisions (e.g. how many cells?) from the beginning of the processing within the data basis. All further analysis steps can be automated then and are of higher quality, the more accurate the processing of the images is. The purpose of this workflow is not to just push the button and apply something like an autopilot (which is not entirely possible so far, even if the data is super-resolved, artifacts outside the cell in the medium can appear). It is far more an adaptive and at every stage of the workflow fully accessible toolbox that helps scientist who works with imaging based data to minimize bias or inconsistencies of the whole procedure until a representative data set is ready to receive more complex analytical procedures. Analytical features shown in the study give a taste of some procedures that could be implemented based on the extracted information. The scope of this workflow is to focus on extraction, transformation and labeling. Once the corrected data satisfies criteria of acceptance by the investigator, further steps of the protocol can be analyzed quickly within the mentioned working days. However, we are convinced that it is important to get the full control about your data. By looking multiple times over generated data, other interesting observations can be made which could lead (like in the presented study) to further proceedings. In other words, the investment of time in correction pays out in enhanced reproducibility, minimizing bias and structured data transformation for further analysis using Celltool or R. The Celltool modeling was conducted using the most simple approach: binary images based on raw grayscale images. However, using T-projected fluorescence micrographs to extract ROIs is also possible and could be a step forward towards a more fully automated segmentation.

##########
3. Both brightfield and fluorescence images were used in this study. However, it is not clear if brightfield and/or fluorescence images were quantified in figures 3-8. It should be mentioned in figure 3-8 captions which set of raw images (brightfield or fluorescence time-lapse recording) did the data come from.
##########

Corrected

##########
4. pp5. "Binary images are sequentially" - The image processing pipeline suggests that the sentence must be clarified logically, e.g. replace "Binary images" term with "Raw grayscale images" term.
##########

Corrected

##########
5. The paper needs more clarification on the image processing and analysis workflow of the fluorescence time lapse images
##########
(Text also added to caption of figure 3. in the paper)

Processing of the fluorescence time lapse recordings is conducted on the basis of cropping the relevant frames until single particle level is reached. Analysis of fluorescence micrographs is based on the measurements defined in ImageJ macros and then further processed using an R pipeline with the mentioned packages. The measurements collected using the ImageJ function can be further used for area comparison in combination with mean gray values and integrated densities. ROI that are collected from binary images that are transformed from raw grayscale images are applied to measure the fluorescence micrographs within the respective cell boundaries. This step eliminates signal that is located outside the ROI. The measured value using ImageJ area refers to respective roi and can be compared with the area results from Celltool. Fluorescence micrographs are used to measure intensities that refer to the protein and vitality situation monitored over time. It is important to know that the raw data does not contain useful meta-data. The workflow enables the experimenter to fully control the annotation of the data in a reproducible way. The outcome should be that after applying the workflow to the fluorescence micrographs to receive properly annotated data tables that can be combined for further analysis using R-packages. Intensity measurements directly correspond to protein levels and dynamics. Data can be therefore used to obtain more perspectives about the observed biological process. Cellular stress can be monitored with different variables containing information for fluorescence activity and morphological changes during stress induction. To monitor the same data from different perspectives makes the analysis more robust and allows to explore the cellular stress response in a more detailed and simultaneous manner in an semi-automated manner. This also helps to re-evaluate the analysis in a well documented manner thus the extraction of information and the processing always starts from the raw data (brightfield and fluorescence micrographs). Further modeling for instance becomes easier thus data is well prepared for more complex analysis tasks. Taken together, the workflow allows to evaluate the observed cellular stress response at protein expression levels (fluorescence microscopy) in a simultaneous and interconnected (ROIs based on Bf) manner with stress response observed by cell shape abnormalities (Celltool).

##########
6. The role of photobleaching needs to be explained.

##

Photobleaching is used through a constant slimfield illumination that quickly bleaches fusion-protein particles towards a single particle level that can be used for the fluorescence micrographs based on T-projections (T for temporal) described in the paper. Slimfield microscopy is used for single molecule localization microscopy and can be used as a super-resolution technique itself (another article covering this specific aspect is going to be published soon). Photobleaching allows to bleach the fluorescent fusion proteins towards a single particle level. From there, images can be reconstructed, processed and analyzed. However, the scope of the presented workflow aims on the extraction, transformation and labeling aspect. The single particle aspect of the data was already in Mayer et al., 2021. With the presented workflow from this paper, other interesting aspects like the inter-connectivity between cell shape and protein expression based on the data set can be explored. Further more, analysis of the data showed that photobleaching of the particles in the cell can be further exploited to extract useful information about the cell vitality represented by the expression levels of the labeled proteins. Photobleaching varies for the monitored proteins at steady-state and under translation stress represented by respective mean gray values accordingly.

##
7. Only sample raw images are made available. Not all screening image source data underlying the results are available to ensure full reproducibility.
##

The data set was updated within the repository.

Competing Interests: No competing interests were disclosed.

Reviewer Report 30 September 2021

https://doi.org/10.5256/f1000research.77023.r93931

Massimiliano Lucidi
Department of Science, Roma Tre University, Rome, Italy

After carefully reading the author's responses, manuscript edits and enrichments, I have no further questions for the authors. Therefore, I consider the proposed work of sufficient scientific quality for indexing in F1000Research.

Is the rationale for developing the new method (or application) clearly explained?

Yes

Is the description of the method technically sound?
Yes

Are sufficient details provided to allow replication of the method development and its use by others?
Yes

If any results are presented, are all the source data underlying the results available to ensure full reproducibility?
Yes

Are the conclusions about the method and its performance adequately supported by the findings presented in the article?
Yes

Competing Interests: No competing interests were disclosed.

Reviewer Expertise: Image processing and bacterial imaging and microscopy

I confirm that I have read this submission and believe that I have an appropriate level of expertise to confirm that it is of an acceptable scientific standard.

Version 1

Reviewer Report 11 June 2021

https://doi.org/10.5256/f1000research.55078.r86409

?

Massimiliano Lucidi
Department of Science, Roma Tre University, Rome, Italy

The authors of the manuscript entitled “Antibiotic Drug screening and Image Characterization Toolbox (A.D.I.C.T.): a robust imaging workflow to monitor antibiotic stress response in bacterial cells in vivo” presented A.D.I.C.T, a workflow based on brightfield microscopy images that covers aspects of experimental setup deployment, data acquisition, image processing and statistical analysis of the *Shewanella putrefaciens* CN-32 cell morphological alterations upon exposure of puromycin-induced protein synthesis arrest.

Although the paper is well structured and suitable for the broader readership of F1000Research,

in my opinion there are few points that should be revised to increase the quality of this manuscript.

Major revisions

1. The authors employed the puromycin antibiotic to analyse bacterial cell morphology modifications. However, this antibiotic is poorly employed to induce morphological alteration in bacteria and has few applications in clinical settings for bacterial infection treatment. On the other hand, many antibiotics induce bacterial cell filamentation at sub-inhibitory concentration such as fluoroquinolones or beta-lactams (Nonejuie *et al*., 2013[1]; Htoo *et al*., 2019[2]). Why did the authors decide to use puromycin instead of other antibiotics? I suggest applying the CellTool-based method to evaluate bacterial morphological modifications induced by other antibiotics.

2. What is the puromycin minimal inhibitory concentration (MIC) of *Shewanella putrefaciens* CN-32? How much below the MIC is the puromycin concentration used in this work (200 µg/ml)?

3. The most effective thresholding algorithms for bacterial image processing are Otsu or Bernsen (Nichele *et al*., 2020[3]). Why did the authors employed 'Percentile' thresholding algorithm? Please justify this choice in the manuscript.

Minor revisions

1. Please substitute "druginduced" with "drug induced" in the Methods section (paragraph: "Biological model system"; line 10).

2. Photobleaching is a phenomenon produced by laser exposure in fluorescence microscopy and it is not a typology of fluorescence microscopy. Please eliminate "photobleaching" in the sentence "Images are acquired using brightfield and photobleaching fluorescence microscopy" from the Methods section (paragraph: "Image acquisition"; line 1) or justify the use of this word in the manuscript.

3. Please add the graph axis titles in Figures 3C and 3D.

4. Please substitute "Further more" with "Furthermore" in the Results section (paragraph: "Proof of concept; Cell shape analysis and modelling"; line 17).

References

1. Nonejuie P, Burkart M, Pogliano K, Pogliano J: Bacterial cytological profiling rapidly identifies the cellular pathways targeted by antibacterial molecules.*Proc Natl Acad Sci U S A*. 2013; **110** (40): 16169-74 PubMed Abstract | Publisher Full Text
2. Htoo HH, Brumage L, Chaikeeratisak V, Tsunemoto H, et al.: Bacterial Cytological Profiling as a Tool To Study Mechanisms of Action of Antibiotics That Are Active against Acinetobacter baumannii.*Antimicrob Agents Chemother*. **63** (4). PubMed Abstract | Publisher Full Text
3. Nichele L, Persichetti V, Lucidi M, Cincotti G: Quantitative evaluation of ImageJ thresholding algorithms for microbial cell counting. *OSA Continuum*. 2020; **3** (6). Publisher Full Text

Is the rationale for developing the new method (or application) clearly explained?

Yes

Is the description of the method technically sound?
Yes

Are sufficient details provided to allow replication of the method development and its use by others?
Yes

If any results are presented, are all the source data underlying the results available to ensure full reproducibility?
Yes

Are the conclusions about the method and its performance adequately supported by the findings presented in the article?
Yes

Competing Interests: No competing interests were disclosed.

Reviewer Expertise: Image processing and bacterial imaging and microscopy

I confirm that I have read this submission and believe that I have an appropriate level of expertise to confirm that it is of an acceptable scientific standard, however I have significant reservations, as outlined above.

Author Response 25 Aug 2021

Benjamin Mayer, Philipps Universität Marburg, Marburg, Germany

Dear Massimiliano Lucidi,

Thank you for reviewing our work. We would like to answer questions and highlight improvements we made with this rebuttal letter.

Major revisions
1. The authors employed the puromycin antibiotic to analyse bacterial cell morphology modifications. However, this antibiotic is poorly employed to induce morphological alteration in bacteria and has few applications in clinical settings for bacterial infection treatment. On the other hand, many antibiotics induce bacterial cell filamentation at sub-inhibitory concentration such as fluoroquinolones or beta-lactams (Nonejuie *et al*., 2013; Htoo *et al*., 2019). Why did the authors decide to use puromycin instead of other antibiotics? I suggest applying the CellTool-based method to evaluate bacterial morphological modifications induced by other antibiotics.

Answer: Raw data used in the workflow was generated during a single molecule tracking study about the SRP-pathway (Mayer *et al.* 2021). There, our initial aim was to investigate SRP-ribosome dynamics but during the study, the appearance of abnormally altered cell morphology was observed and subsequently quantified using the A.D.I.C.T. workflow in order to systematically explore these changes. We applied puromycin, rifampicin and

chloramphenicol (see figure 6 in the updated version) for inhibitory experiments studying protein-biosynthesis dynamics at single molecule levels. Puromycin is relatively affordable, available and not relevant for medical usage. Data based on puromycin stressed cells serves in this study as a control used for protein-biosynthesis inhibition because it is known to lead to premature peptide chain termination at the peptidyl-transferase site in the 50S ribosomal subunit (reviewed by Aviner in 2020).

2. What is the puromycin minimal inhibitory concentration (MIC) of Shewanella putrefaciens CN-32? How much below the MIC is the puromycin concentration used in this work (200 µg/ml)?

Answer: With respect to the minimal inhibitory concentration, there is no information available for *S. putrefaciens*. According to general supplier informations, puromycin is weakly active against Gram-negative organisms and for E. coli, 100 µg/ml are recommended. In order to apply sufficient antibiotic stress, we used double of the recommended concentration and applied viability screenings simultaneously to each conducted experiment using serial dilutions to check if the cell response was sensitive enough towards puromycin exposure. Our results show that *S. putrefaciens* cells are susceptible towards puromycin at respective concentration on a sublethal basis (see fig 4B). To our knowledge, results show for the first time, how much puromycin could be used in order to induce sublethal cell-stress in *Shewanella putrefaciens.* However, further improvements of the workflow are also connected to more detailed experiments (e.g. different concentrations) and data-acquisition strategies. We therefore agree that different antibiotics with respective modes of action could be explored in more detail, but that would exceed the scope of this paper showing only a monitoring method focused on delivering useful information about the samples by using very basic and therefore broadly available imaging techniques.

3. The most effective thresholding algorithms for bacterial image processing are Otsu or Bernsen (Nichele *et al.,* 2020). Why did the authors employed 'Percentile' thresholding algorithm? Please justify this choice in the manuscript

Answer: Regarding the usage of implemented thresholding algorithms, 'Percentile' was used because it is considered as the most robust tool for this specific purpose. 'Percentile' showed for this particular data set the best background detection without affecting cell areas on average. We added figure 2 to the Area outside cells is corrected manually thus regular brightfield images are used. The decision for this particular thresholding algorithm felt after comparing all thresholding algorithms using the 'Try all' function implemented in FIJI. As mentioned in the text, more advanced microscopy techniques (e.g. phase contrast) could give better images for thresholding and segmentation. Further more and not yet covered by this method paper, projections themselves can be used to detect and to compare drug stressed cell populations according to their shape. We however focused on the most simple imaging technique (brightfield) thus the aim of the study is to show how useful information gain can be established with the presented workflow. We agree with the idea that there are a lot more interesting experiments that could (and should) be conducted to address similar biological questions. We therefore hope that the presented workflow might empowers other investigators in establishing similar pipelines in order to increase

reproducibility of their research and exploit their data as versatile and efficiently as possible.

References:

Aviner, Ranen. "The science of puromycin: From studies of ribosome function to applications in biotechnology." Computational and structural biotechnology journal vol. 18 1074-1083. 24 Apr. 2020, doi:10.1016/j.csbj.2020.04.014

Mayer B, Schwan M, Oviedo-Bocanegra LM, Bange G, Thormann KM, Graumann PL. Dynamics of Bacterial Signal Recognition Particle at a Single Molecule Level. Front Microbiol. 2021 Apr 30;12:663747. doi: 10.3389/fmicb.2021.663747. PMID: 33995327; PMCID: PMC8120034.

Competing Interests: No competing interests were disclosed.